Determining the interaction matrix using starlight

François Wildi[*a,b], Guido Brusa[b]
[a] West Switzerland University of Applied Science, EIVD, 1400 Yverdon, Switzerland
[b] Steward Observatory, University of Arizona, Tucson AZ85721

ABSTRACT

The adaptive optics system of the 6.5m MMT, based on a deformable secondary mirror has been of the sky now for 6 runs of roughly 2 weeks each[2,3,4]. Altogether its performance has been quite satisfactory with a crop of science results[1,5,6] . However, even if the mirror has shown it promises, it has proven difficult to improve the system in terms of wavefront quality much beyond what it achieved during 1st light. In particular, it has not been possible to improve image quality by using a larger number of modes than the 52 modes used originally. One reason for this behavior could be that the interaction matrix used to build the AO controller has been measured in lab conditions using a different optical set-up than the one on the telescope. In a Cassegrain adaptive secondary AO system measuring the interaction matrix in the way all other AO systems do is impossible when the secondary is mounted on the telescope. In this paper, we present a way of measuring the interaction matrix on the telescope using real natural guide stars as sources. We present simulations results that show that this method can be used to measure the interaction matrix to a high signal-to-noise ratio.

Keywords: Adaptive optics, voice-coil deformable mirror, system calibration

INTRODUCTION

The success of the MMT adaptive optics system using the world's first adaptive secondary mirror has sparked a lot of interest from the teams building large telescope AO systems. However, the present lack of possibility to measure the interaction matrix once the system is installed on the telescope is a big concern, because it can severely limit the quality of the correction and/or the number of modes with which the optical loop can be stably closed and limit the investigation possibilities in case of problems

1. WHAT IS THE PROBLEM?

Traditional AO systems are compact instruments that are contained within a single housing located around the telescope focus telescope. The deformable mirror (DM) is located in the AO system behind this first focus (see figure 1, right).
On those systems, it is straightforward to measure the interaction matrix $\mathbf{D}$' by obstructing the telescope beam and inserting an artificial star at the 1st focus location. The mirror modes $\vec{m}_i$ are excited one after another and the wavefront sensor signal $\vec{s}_i$ that each mode produces is recorded. The concatenation of these signals *is* the interaction matrix $\mathbf{D}$' (in modal representation). The pseudo inverse $\mathbf{D}_+$ of this matrix is called the reconstructor. Given an arbitrary slope vector $\vec{\mathbf{s}}_j$, the modal decomposition of the wavefront is the product $\mathbf{D}_+\vec{\mathbf{s}}_j$.

As the left part of figure 1 below shows, there is no intermediate focus where to place an artificial star upstream of the DM in an Cassegrain adaptive secondary system, and thus, no way of measuring **D'** once the system is on the telescope. This could be made be adding projections optics in front of the secondary to that would change to beam path a defeat the purpose a the calibration). On the other hand the need for calibration is rendered more acute given the fact that the AO system is assembled on the telescope for each run and subsequently taken apart after the run, unlike traditional AO system that are made of a single mechanical unit. Today, the MMT-AO system relies on an interaction matrix taken in

[*] Send correspondence to *francois.wildi@eivd.ch; phone ++41 24 4232 305;

the laboratory[9], with no provision to compensate for registration or design errors, and embedding the possible effects of the optical bench used for calibration

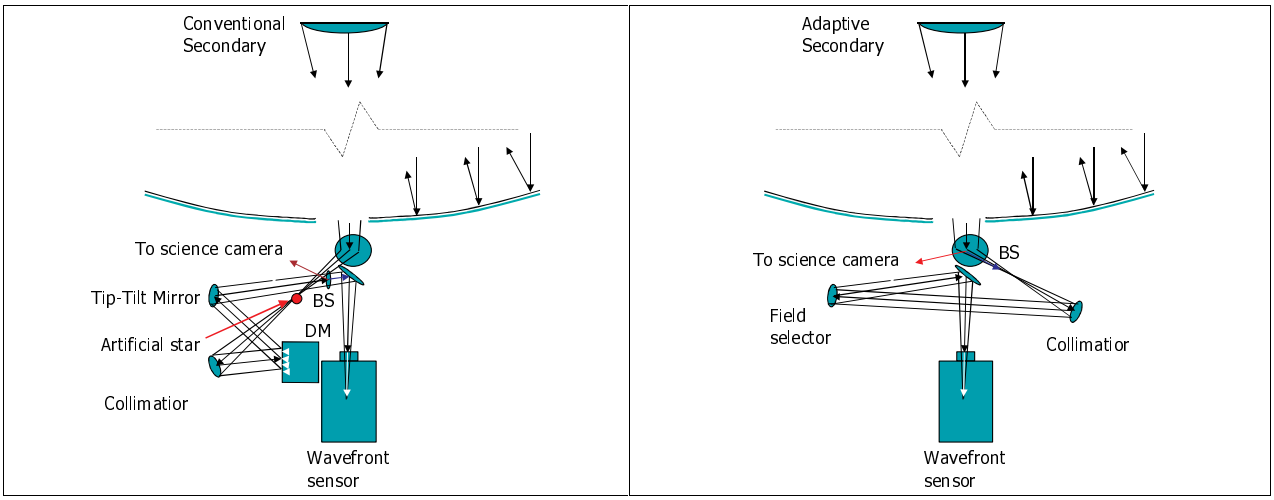

Fig 1: in adaptive secondary system There is no focus from where the DM can be illuminated in adaptive secondary system (right) this is not the case unlike in a traditional AO system (left). In order to illuminate the secondary and auxiliary optics must be used. Note that a Cassegrain telescope is shown. In a Gregorian telescope the presence of an intermediate focus simplifies the optics.

2. THE SOLUTION WE PROPOSE

To compensate for the lack of artificial star producing a good quality wavefront to illuminate the DM, we propose to *using a seeing limited wavefront from a natural guide star* (NGS) to perform the measurement of the interaction matrix of the AO system when assembled on the telescope, with the obvious problem that the available wavefront has not even closely the quality and the stability required for this measurement.

2.1. Open loop approach

One can think for several ways to perform the interaction matrix measurement with an NGS, the most obvious of which is to illuminate the Adaptive Secondary with the NGS, impose a known distortion on the DM and measure the wavefront sensor (WFS) signal induced. This is what we call the 'open loop approach'. There are severe problems associated with this approach:

- The WFS has a limited range and it is linear only for small aberrations. Most WFS's designed for AO operation are not even linear for normal open-loop seeing conditions, because they are designed for sensitivity not for range. Introducing a wavefront distortion of sufficient magnitude for the measurement of the interaction magnitude will definitively drive the WFS out of its linear range if not out of its operating range
- In open loop, the averaging of the turbulence-induced noise on the WFS is subject to the atmospheric statistics, whose energy is mostly located in the low frequencies (see figure below). This implies that the averaging of the WFS signal does have to be made over long periods of time and that the calibration of the interaction matrix will be a lengthy operation

2.2. Closed-loop approach

In close loop, the 2 drawbacks mentioned above disappear:

- After AO correction the apparent r0 is much larger than the atmospheric seeing and therefore, the WFS works in the small signal linear regime[1]. Moreover, adding distortion on the mirror will not affect the operating point of the WFS since the AO system will impose an average null signal on the WFS.
- In close-loop, the spectral density of the noise seen by the WFS is the product of the spectral density of the atmospheric statistics times the rejection function of the AO loop, which has a high pass behavior.

However, for this technique to work, we must assume that we have an interaction matrix whose accuracy is at least sufficient to have stable close-loop operation. We will accept this assumption throughout this communication, and this is why we call our technique 'calibration' rather than 'measurement' of the interaction matrix.

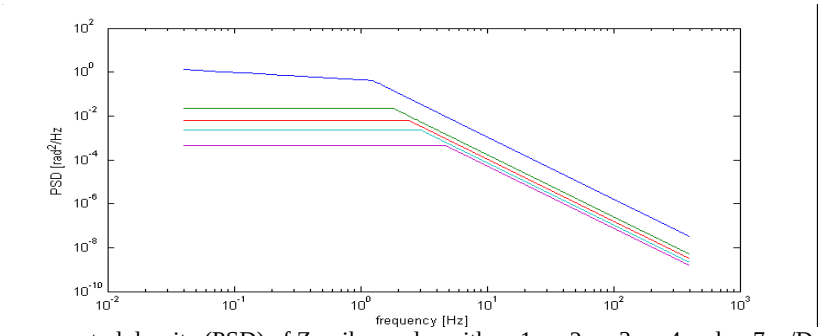

Fig 2: Temporal Power spectral density (PSD) of Zernike modes with n=1, n=2, n=3, n=4 and n=7. v/D_0=1.2 (From ref.10)

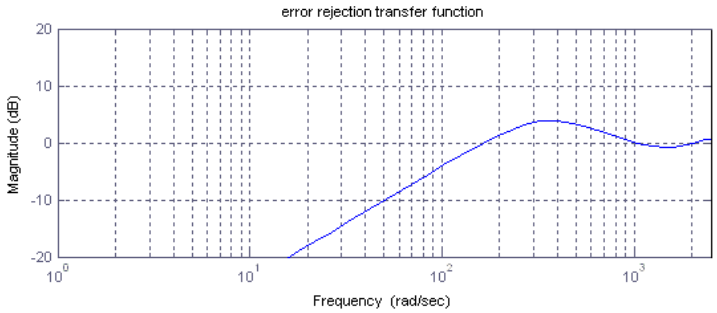

Fig 3: Rejection function of a closed-loop AO system. (integrator @ f_s=800 [Hz], LBT AO DM dynamics)

2.3. Lock-in approach

With the close-loop, we have a way of introducing a stimulus in the AO system. This stimulus is the distortion imposed on the mirror which we will call the 'mode' $\vec{m}$. To improve the SNR we could obtain with the closed-loop approach, we propose to use a technique well-known to the signal recovery community: Using an AC stimulus and a phase-locked measurement of the signal produced. With respect to the closed-loop approach we expect the following advantages:

- Concentration of the stimulus power on a single frequency that can be pushed beyond the corresponding modal bandwidth in the atmosphere.
- Doubling of the possible input signal. At low spatial frequencies, the input signal is limited by the capture range of the AO system and at high spatial frequencies, it is limited by the stiffness of the mirror modes
- Symmetrysation of the operating point of the DM
- Clear elimination of low frequency effects like temperature, seeing, gravity and other telescope related phenomena.

[1] Actually, for reasons beyond the scope of this paper, the amount of power left in the wavefront after AO correction goes down faster than the power of the WFS signal.

3. LOCK-IN ANALYSIS

3.1. Principles

Let us look at the AO-loop diagram below, and consider the static response: If a distortion of the DM is introduced in the system (blue arrow), it will feed back onto the WFS and the controller will cancel it a much a it can. Therefore, the distortion related WFS signal will vanish and the distortion will be corrected back. In other words, the calibration cannot be performed in the customary way, since that method relies on the WFS signal produced for a certain DM distortion.

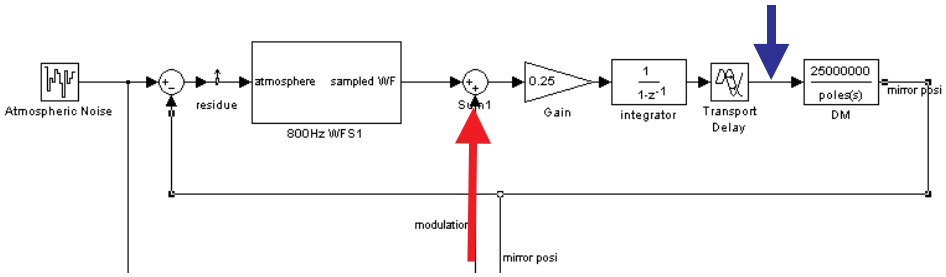

Fig 4: AO-loop diagram with the proposed modulation scheme

If, on the other hand, a bias $\vec{\mathbf{s}}_{bias}$ is added to the WFS signal (red arrow), the AO controller will generate a DM command such that the sum of the WFS signal $\vec{\mathbf{s}}_{WFS}$ and $\vec{\mathbf{s}}_{bias}$ is null (formally, $(\vec{\mathbf{s}}_{WFS} - \vec{\mathbf{s}}_{bias})$ belong to the nullspace of D_+). Without the bias, the DM command is such that $\vec{\mathbf{s}}_{WFS}$ is null and thus the position difference $\hat{\vec{\mathbf{m}}}_{bias}$ induced by the slope bias is the opposite than the one that would produce a signal $\vec{\mathbf{s}}_{bias}$ on the WFS.

This method, rather than producing the matrix $\mathbf{D}'$ by looking at the WFS signal produced by the known modal excitation of the DM, *measures directly the reconstructor matrix* $\mathbf{D}_+$ from a sequence of $\vec{\mathbf{s}}_{bias}$. I.e. it measures the modal effect on the DM of a WFS signal vector. By iterating on an arbitrary number of modes, the complete DM modal space can be covered. It must be said that the voice-coil adaptive secondary lends itself particularly well to this measurement, since each actuator has a position sensor collocated with it and a local servo loop, that make the actual position of the actuator available to a high accuracy[7,8].

$$\begin{aligned} \vec{s}_{bias\,1} &\rightarrow -\hat{\vec{m}}_{bias1} \\ \vec{s}_{bias\,2} &\rightarrow -\hat{\vec{m}}_{bias2} \\ &\vdots \\ \vec{s}_{bias\,n} &\rightarrow -\hat{\vec{m}}_{bias\,n} \end{aligned}$$

We choose to stimulate the loop with the set of nominal modal slope vectors $\vec{\mathbf{s}}_{bias} = \vec{\mathbf{s}}_{1..n}$, i.e. the slopes produced in the lab during the initial measurement of the interaction matrix so that the calibrated reconstructor $\hat{\mathbf{D}}_+^*$ can be calculated from the original reconstructor $\mathbf{D}_+$ by

$$\hat{D}_+^* = \begin{bmatrix} -\hat{\vec{m}}_{bias\,1} & -\hat{\vec{m}}_{bias\,2} & \dots & -\hat{\vec{m}}_{bias\,n} \end{bmatrix} D_+$$

3.2. Signal

The slope bias injected is multiplied by a symmetric AC modulation function. This is our input signal which is a time-varying slope vector. The output signal is the mirror position defined in the actuator space. The part of this position that is due to turbulence correction is considered noise, because we are interested in the relationship between the bias slope vector and the mirror position change it produces. The injection of the modulated slope bias is called modulation.
During modulation the mirror position is multiplied by the input signal properly phased to best match the phase lag of the servo loop. We study the properties of the output signal.

We choose to modulate the signal bias $\vec{\mathbf{s}}_{bias}$ by square wave for operational simplicity. This wave is the sum of odd harmonics of the original frequency, each one being filtered by the closed-loop response of the AO-loop.
After modulation of the system response by the input signal, the 1st harmonic of the response is folded back to DC, while the higher odd harmonics become even harmonics. A simple averager with a window of $T_{AC}/2$ will suppress all these harmonics, leaving only the DC component:

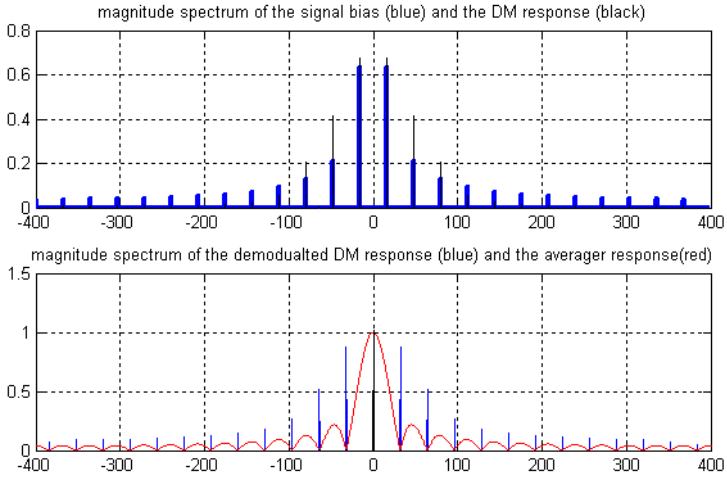

Fig 5 : Power spectra of the modulation and the AO loop response (top, in blue, respectively black). Power spectra of the demodulated mirror position before and after averaging (bottom, in blue, respectively red)

3.3. Noise budget

As mentioned, the noise is the mirror position induced by the atmospheric correction. A modal expansion of the turbulence is performed and the temporal spectrum of each mode is analysed separately during the lock-in operations: The PSD of the atmospheric noise is given in ref. 10. When measured as a mirror displacement, this PSD has been filtered by the AO system rejection function (unlike the modulation which is filtered by the AO system closed-loop transfer function). The mirror position 'noise' will be submitted to the demodulation, which will translate in the frequency domain into a convolution by the harmonic spectrum of the modulation signal. Subsequently, it is filtered by the averager. The figure 6 below presents an example for a Z=2.

On the DM, the noise from all modes will add up in the error budget. To compute the total noise PSD N(f) on the DM, we have made a numerical quadratic sum of the modal PSD's up to mode 250, taking into account each mode's specific bandwidth and energy. This PSD is presented in the figure 7 below. The 2nd curve on that figure is the noise power P(f) within the bandwidth 0 to f.

$$P(f) = \int_0^f N(f)df$$

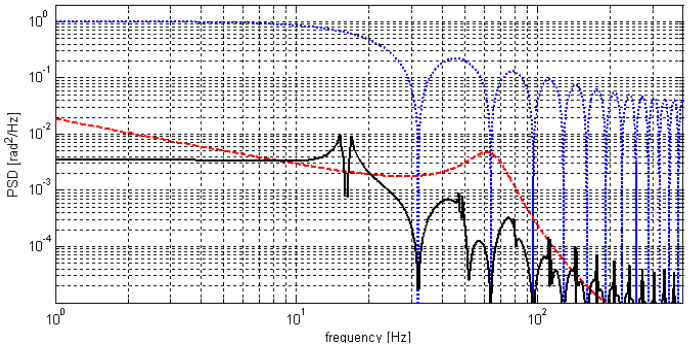

Fig 6 : Modal PSD for Z=2 and v/D=1.2 (dashed), transmittance of the averager (blue) and output noise (black). Note that the spectral window is already beyond the modal cut-off frequency of the modal PSD, hence the negative slope to the left of the controller resonance peak

Since selecting a measurement integration time T will determine the lower bound of the frequency selectivity, one can use P(f) to determine to SNR obtainable after an integration of T, knowing the input signal power. Conversely, one can determine the T required to guarantee a certain measurement SNR. (Remember that the bandwidth of the low path filter is inversely proportional to the measurement time).

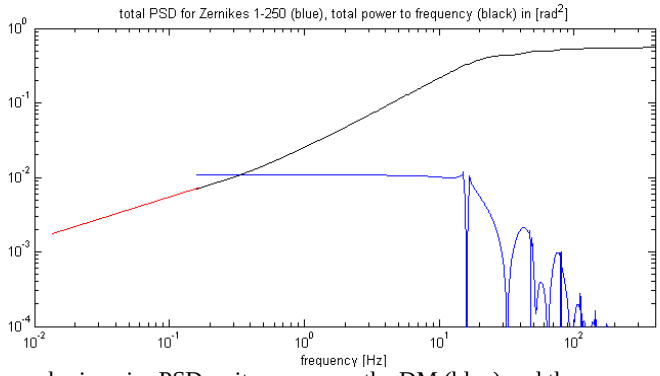

Fig 7 : The atmospheric noise PSD as it appears on the DM (blue) and the same curve integrated up to the frequency given on the x-axis (black and red)

4. SIMULATIONS

We have performed a number of simulations to prove the lock-in calibration concept. The results we present below were obtained with the model of a system, running f_s= 800 Hz with Zernike modes orthogonalized on the pupil. The input signal modulation was 1 [rad] @ V at 16Hz with a wind speed of 30m/s, r0=0.16m and D=8.2m. The reconstructor used was the ideal D+ and no reconstructor error were assumed. Under these conditions, were expecting to see $\hat{\mathbf{D}}_{+}^{*} = \mathbf{D}_{+}$: The mode $\hat{\vec{\mathbf{m}}}_{bias\,n}$ exhibited by the mirror when the slope vector $\vec{\mathbf{s}}_{bias\,n}$ is applied as bias should be $\vec{\mathbf{m}}_{n}$.

Each mode is identified separately by modulation the slope error with the proper slope bias. Therefore the modulation time (i.e. the number of modulation cycles) in an important parameter, because, once multiplied by the order n of the system, it can lead to very long simulation times but also to inaccetably long calibration time on the telescope. The results we present below where obtained with modulation times equivalent to 50 s/mode on the telescope which might be longer than what can be accepted on a real high order system. Figure 11 below shows the SNR as a function of modulation time

Fig 8: The WFS signal is biased by the slope vector corresponding to the Zernike tilt. After 800 cycles (50s) of AC stimulation, the deformable mirror position offset is essentially a pure tilt as can be seen in the top r/h figure representing the demodulated DM modal position v.s. mode number. At that point the tracking error seen by the WFS is completely averaged and the tracking error variance does reflect the Noll residuals as filtered by the controller (bottom r/h figure).
The mode estimated has an rms error of 2% with respect with the original mode, with a clear edge roll-off along one of the diagonals.

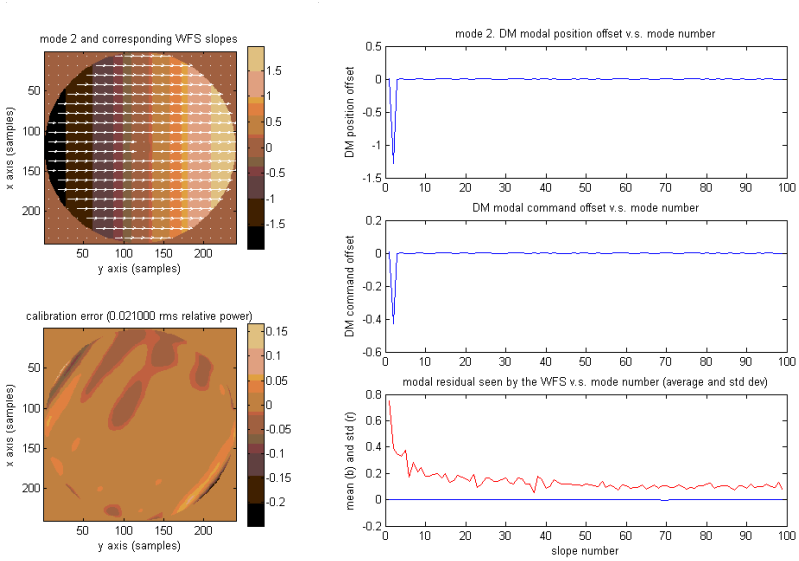

Fig 9: The WFS signal is biased by the slope vector corresponding to the Zernike astigmatism. As with tilt, after 800 cycles of AC stimulation, the DM position offset is almost pure a pure astigmatism (top r/h figure). Again, the tracking error seen by the WFS is completely averaged and the tracking error variance does reflect the Noll residuals as filtered by the controller (bottom r/h figure).
The mode estimated has an rms error of 2.7% with respect with the original mode, with a clear edge roll-off along the same diagonal as the case presented on figure 8.

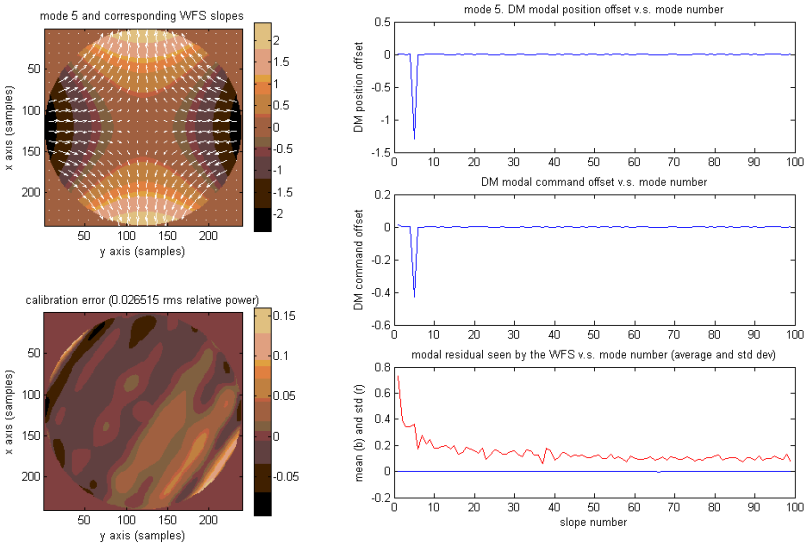

Figures 8 and 9 present the result of the calibration of the tilt and astigmatism . They show a systematic error in the wavefront estimation that is made of a diagonal tip/tilt component and diagonal edge roll-off. The possible sources for these errors have not been yet investigated but we think that a problem with the model of the Shack-Harmann wavefront sensorcan be the source of the tip-tilt error. The most likely source for the edge roll-off is the fact that sub-apertures with less than 50% illumination were discarded in this simulation, penalizing in particular the pupil edge area that is located along the diagonal of the lenslets lattice.
Figures 10 and 11 present the same information for Zernike modes 70 and 99. Here also the error seems to be made of the same components as before with visible diagonal tip/tilt and edge roll-off. However, the edge roll-off seems to have lost its diagonal feature and in the case of mode 99, clearly shows a residual of the original mode which could be the sign of an important open loop gain error. Indeed, if the gain of the system is to low, it will not correct the bias properly at the modulation frequency. This is a likely possibility since mode 99 has edge features that are beyond the Nyquist frequency of the lenslet lattice and that are therefore not properly measured by the WFS. To avoid this effect, a base of Karhunen-Loeve modes will be used in the future, to take advantage of its smoother edges.

Fig 10: The WFS signal is biased by the slope vector corresponding to the Zernike mode 70. After 800 cycles of AC stimulation, the DM position offset is still made mostly of Zernike mode 70 (top r/h figure) but it does show a significant amount of noise. As before the tracking error is averaged.
The mode estimated has now a significant rms estimation error of around 13% with respect with the original mode, with a tip/tilt contribution superposed with edge roll-off.

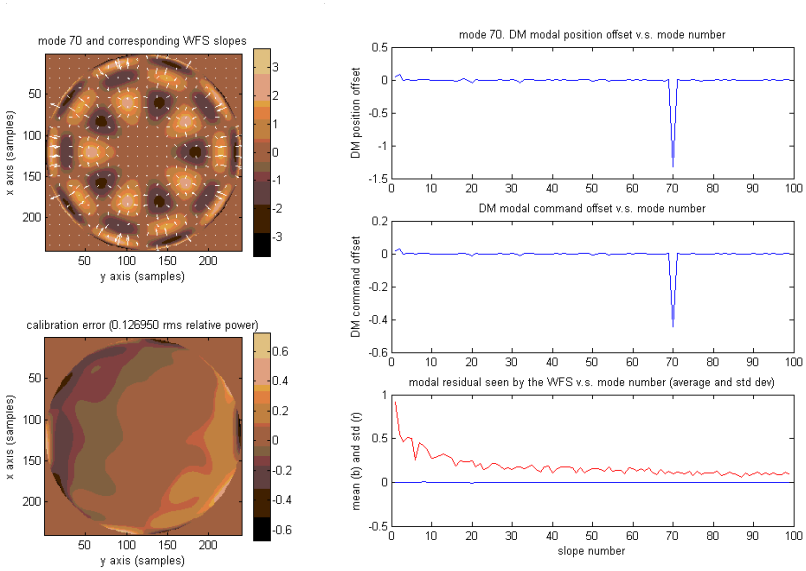

Fig 11: The WFS signal is biased by the slope vector corresponding to the Zernike mode 99. After 800 cycles of AC stimulation, the DM position offset is still made mostly of Zernike mode 99 (top r/h figure) but it does show a significant amount of other modes. Unlike for lower order modes, the tracking error does show positive correlation with the modal amplitude errors. As if there was some coupling between the stimulated mode and others compounded with low gain on the latter
Like mode 70, this mode is estimated with significant rms error of around 13% with respect with the original mode, with a tip/tilt contribution superposed with edge roll-off.

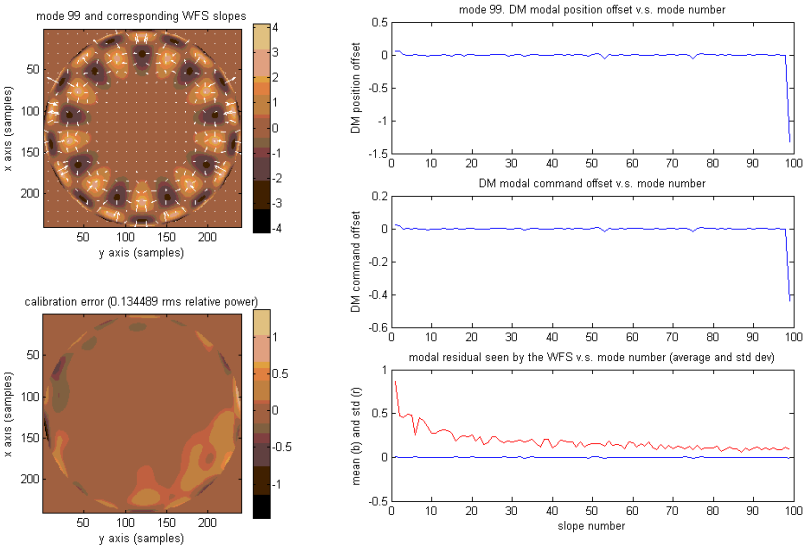

The behaviour of the calibration errors versus calibration time has also been investigated is shown on fig. 12. This error follows approximately the behaviour derived numerically (fig 7) but only for Zernike modes of low order. For higher order modes, the error stays above the predicted level and it levels off at a level that increases with the mode number. This behaviour severely limits the useability of the method for all but the first few 10's of modes in the system considered and it is not well understood at this time.

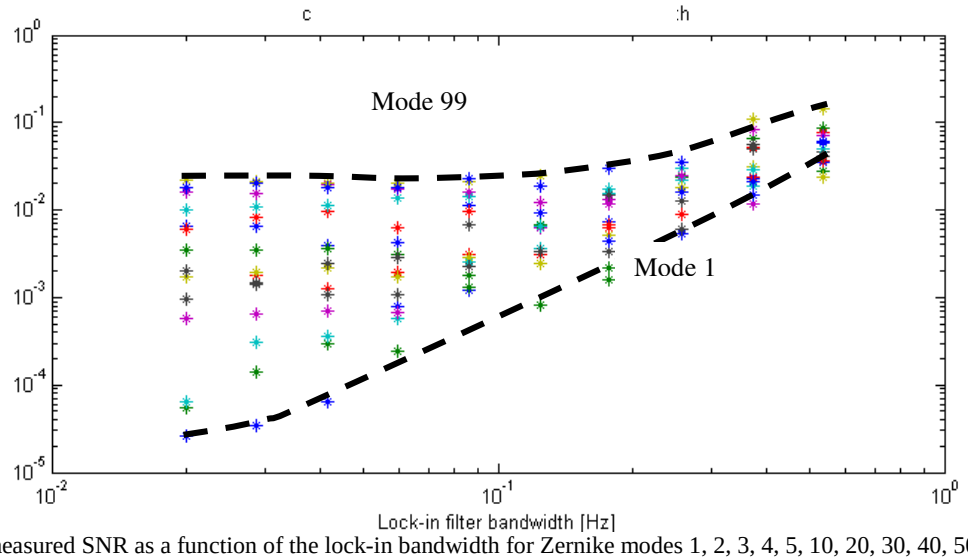

Figure 12: The measured SNR as a function of the lock-in bandwidth for Zernike modes 1, 2, 3, 4, 5, 10, 20, 30, 40, 50, 60, 70, 80, 90 and 99. While the calibration error of the low order modes follows the law obtained numerically (fig 7), the error of high order modes levels off at a much higher values, limiting the accuracy of the calibration

5. CONCLUSION

At this point, even if the analysis of the calibration problem looks promising, the simulations have shown performance limitations. While some of them seem to be due to modeling problems or the use of an inappropriate modal base, there might be more fundamental limitations. The limit in SNR observed on high order modes could mean that the approach considered could only be used on adaptive secondary multi-DM systems, for which the adaptive secondary is only a modest order corrector, but not on high order on-axis systems. More research need to be performed to understand the source of this limitation.

This research is on-going and the next step will be to evaluate the behaviour of the calibrated reconstructor in closed loop and iterate the calibration to see if (and at what level) the calibration stops degrading the previous reconstructor estimation. Then, we will introduce reconstructor errors to observe an actual improvement through calibration.

There are areas that need to be investigated like the way of introducing new modes on the system that were not measured in the laboratory or do not have a sable behaviour in the closed loop.

ACKNOWLEDGMENTS

F. Wildi is partly funded by the European Southern Observatory for this work

REFERENCES

1. M. A. Kenworthy, D. Miller, P. Hinz, G. Brusa, L. Close, D. McCarthy, Jr., D. Fisher, M. Lloyd-Hart, F. Wildi, “Scientific results from the MMT natural guide star adaptive optics system”, this conference [5490-48]
2. F. Wildi, G. Brusa, A. Riccardi, M.. Lloyd-Hart, L. Close. “1st light of the Adaptive optics system at the 6.5m MMT”, SPIE international symposium on Optical Science and technology, 4-5 August 2003, San Diego CA, USA, (5169-03)
3. G. Brusa, A. Riccardi, F. Wildi, M. Lloyd-Hart, H. Martin, R. Allen, D. Fisher, D. Miller, P. Salinari, R. Biasi, D. Gallieni, and F. Zocchi. “MMT adaptive secondary: First AO closed-loop results”, SPIE international symposium on Optical Science and technology, 4-5 August 2003, San Diego CA, USA (5169-04)
4. M.. Lloyd-Hart , F. Wildi, G. Brusa, “Lessons learned from the first adaptive secondary mirror”, SPIE international symposium on Optical Science and technology, 4-5 August 2003, San Diego CA, USA (5169-10)

5. “Mid-infrared images of post AGB star AC Herculis with the MMT Adaptive optics system”, L. Close, B. Biller, W. Hoffmann, P. Hinz, J. Bieging, F. Wildi, M. Lloyd-Hart, G. Brusa, D. Fisher, D. Miller, R. Angel. ApJ letters, November 20, 2003 issue.
6. “High resolution images of orbital motion the trapezium cluster: first scientific results from the MMT deformable secondary mirror adaptive optics system”. L. Close, F. Wildi, M Lloyd-Hart, G. Brusa, D. Fisher, D. Miller A. Riccardi, P. Salinari, D. McCarthy, R. Angel, R. Allen, H. Martin, R. Sosa, M. Montoya, M. Rademacher, M. Rascon, D. Curley, N. Siegler, W. Duschl. Astrophysical Journal, 599, 2003
7. F. Wildi, G. Brusa, D. Miller, D. Fisher, R. Allen, M.. Lloyd-Hart, A. Riccardi, H. Martin. “Towards 1st light of the 6.5m MMT adaptive optics system with deformable secondary mirror”, SPIE Conference on Astronomical Telescopes and Instrumentation, 22-28 August 2002, Waikoloa, Hawaii, USA. (4839-19)
8. A. Riccardi, G. Brusa, C. Del Vecchio, R. Biasi, M. Andrighettoni, D. Gallieni, F. Zocchi, M. Lloyd-Hart, F. Wildi, H. M. Martin “The adaptive secondary mirror for the 6.5 conversion of the MMT”, Beyond conventional adaptive optics”, Venezia 2001, eds. R. Raggazzoni et S Esposito.
9. P.C. McGuire, M. Lloyd-Hart, J.R.P. Angel, G.Z. Angeli, R.L. Johnson, B.C. Fitzpatrick, W.B. Davison, R.J. Sarlot, C.J. Bresloff, J.M. Hughes, S.M. Miller, P. Schaller, F.P. Wildi, M.A. Kenworthy, R.M. Cordova, M.L.Rademacher, M.H. Rascon, J.H. Burge, B.L. Stamper, C.Zhao, P. Salinari, C.Del Vecchio, A. Riccardi, G.Brusa, R. Biasi, M. Andrighettoni, D. Gallieni, C. Franchini, D.G. Sandler, T.K. Barrett,” Full-System Laboratory Testing of the F/15 Deformable Secondary Mirror for the New MMT Adaptive Optics System”, SPIE Conference on Adaptive Optics Systems and Technology, ed s. R.Q. Fugate and R. K. Tyson, 3762, 28-37, Denver, 1999.
10. J.-M. Conan, G. Rousset, P.-Y. Madec “Wave-front temporal spectra in high-resolution imaging through turbulence”, JOSA A, Vol 12, No7, 07.95.